

Article

Modeling of 1,2-Dibromoethane Biodegradation in Constant Electric Field

Petya Popova-Krumova, Venko Beschkov *, Evgenia Vasileva and Tsvetomila Parvanova-Mancheva

Laboratory of Chemical & Biochemical Reactors, Institute of Chemical Engineering, Bulgarian Academy of Sciences, 1113 Sofia, Bulgaria

* Correspondence: vbeschkov@iche.bas.bg; Tel.: +359-898-447-721

Abstract: This study proposes a mathematical modeling approach for evaluating the effect of applying a permanent electric field on the biodegradation of 1,2-dibromoethane by bacterial cells of *Bradyrhizobium japonicum* 273. Two models for inhibited microbial growth including product inhibition were composed—one using the Monod–Yerusalimsky approach and another one—the Levenspiel kinetic equation. The models were used to process own experimental data obtained without an electric field and ones obtained at the application of an electric field. The experiments were carried out at an optimum anode potential of 0.8 V vs. the standard hydrogen electrode (SHE). Three initial concentrations of substrate were tested: 0.05, 0.1, and 0.15 g dm⁻³. The modeling takes into account the product inhibition on microbial growth assuming 2-bromoethanol as the first biodegradation product. It was found that the positive effect of the electric field is the enhancement of microbial growth, expressed by the increase in the maximum specific growth rate and the increase in the inhibition constant when the model of Monod–Yerusalimsky is applied. The main effect of the electric field is in the increase in the rate constant of 2-bromoethanol removal by electrochemical oxidation, enabling the enhancement the microbial growth and substrate conversion to the product. The obtained results show that the application of a permanent electric field leads to a higher electrochemical oxidation rate (with a rate constant up to 60% higher than for the control experiments) and complete substrate and 2-bromoethanol biodegradation. The model of Levenspiel is not so sensitive to the effects of the electric field on product inhibition.

Keywords: 1,2-dibromoethane; biodegradation; permanent electric field; mathematical modeling



Citation: Popova-Krumova, P.; Beschkov, V.; Vasileva, E.; Parvanova-Mancheva, T. Modeling of 1,2-Dibromoethane Biodegradation in Constant Electric Field. *ChemEngineering* **2022**, *6*, 62. <https://doi.org/10.3390/chemengineering6040062>

Academic Editor: George Z. Papageorgiou

Received: 2 July 2022

Accepted: 3 August 2022

Published: 8 August 2022

Publisher's Note: MDPI stays neutral with regard to jurisdictional claims in published maps and institutional affiliations.



Copyright: © 2022 by the authors. Licensee MDPI, Basel, Switzerland. This article is an open access article distributed under the terms and conditions of the Creative Commons Attribution (CC BY) license (<https://creativecommons.org/licenses/by/4.0/>).

1. Introduction

One of the most commonly detected contaminants in groundwater is 1,2-dibromoethane (1,2-DBE). Today, 1,2-DBE can still persist in groundwater at high levels at some contaminated sites, even though its usage was banned in gasoline and agriculture in the 1980s in Canada, Sweden, and the USA [1].

1,2-DBE was used primarily as an antiknock additive to gasoline and is one of the most effective and widely used pesticide soil fumigants [2]. However many years after its last known application as a soil fumigant, residual 1,2-DBE is still found at remarkably high concentrations in soil because it strongly interacts with the soil matrix [3,4]. 1,2-DBE can slowly leak from such contaminated soils to groundwater over exceedingly long periods, and because of its slow chemical conversion in an aqueous milieu, it is a continuous source of contamination of water supplies [4], even decades after its last use [4,5]. More than 100 formulated pesticides contain 1,2-DBE. In 1977, 120 million kilograms were produced in the United States.

1,2-DBE is highly toxic and probably carcinogenic in humans, and it can lead to damage to the stomach, reproductive system, respiratory system, and nervous system in mammals [6]. 1,2-Dibromoethane affects liver microsomes, DNA, and sperm. Human exposure to 1,2-DBE can cause eye, skin, and respiratory irritation as well as damage to the liver, kidney, spleen, and lungs [7].

1,2-DBE can be characterized by relative hydrophilia, poor bioavailability, and extremely low natural attenuation rate ($t_{1/2} = 17.33$ years) in groundwater [8].

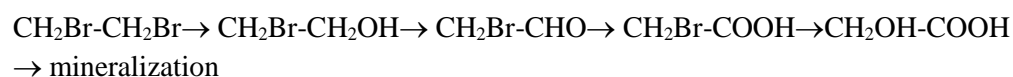
1,2-Dibromoethane is one of many potentially carcinogenic compounds to which humans are exposed. The purpose of the study [9] was to evaluate biochemical mechanisms by which 1,2-dibromoethane might be acting as a carcinogen and by which it might be activated and inactivated.

The Agency for Toxic Substances and Disease Registry maintains a prioritized list of the compounds most commonly found at Superfund sites that pose the most significant potential threat to human health. 1,2-Dibromoethane (ethylene dibromide) ranks sixth among halogenated aliphatic compounds, while 1,2-dichloroethane (1,2-DCA) ranks fourteenth. 1,2-DBE has the second lowest maximum contaminant level (MCL = 0.05 $\mu\text{g/L}$) in drinking water among all organic compounds after dioxin [10].

The biological degradation of 1,2-DBE has been studied under both aerobic [11–14] and anaerobic conditions [15]. It was established that 1,2-dibromoethane and its products, particularly 2-bromoethanol, are toxic to *Xanthobacter autotrophicus*, GJ10 being the most exploited strain for 1,2-dichloroethane biodegradation [8,9]. For the success of any bioremediation process, it is necessary to understand the behavior of microbial populations responsible for the degradation of the targeted contaminants.

In the study by Skopelitou et al. [16], different *Rhizobium* strains were screened for their ability to produce stable and active 1,2-dibromoethane-degrading dehalogenase. Among them, *Bradyrhizobium japonicum* appears to produce the most stable enzymes for 1,2-DBE biodegradation [17]. We shall assume the following main scheme of 1,2-DBE biodegradation shown below.

The biodegradation passes through very toxic intermediates, e.g., 2-bromoethanol and bromoacetaldehyde (cf. Scheme 1) and that is why the complete biodegradation was not observed at higher substrate concentrations above 0.1 g/L. Full dehalogenation was observed below this concentration corresponding to stoichiometric values of released bromide ions.



Scheme 1. Pathway of oxidative biodegradation of 1,2-dibromoethane.

In a previous study, we investigated the biodegradation of 1,2-dibromoethane with *Bradyrhizobium japonicum* 273 cells in presence of a constant electric field [18]. The electric field was applied in order to accelerate the process of oxidation of the intermediate product 2-dibromoethanol. The positive effect of the electric field was proved on the basis of biomass growth and the release rate of bromine for a certain period of time. When no electric field was applied the biodegradation was impeded. It stopped before one bromide atom in the substrate molecule was released completely, i.e., before the complete conversion of 1,2-DBE into 2-bromoethanol. The constant electric field leads to complete degradation and the concentration of bromide ions in the medium reaches stoichiometric values. However, a question arises on the nature of this effect: suppression of product inhibition of microbial growth, enhanced removal of the inhibitor, i.e., 2-bromoethanol by its depletion to further products because of electrochemical oxidation (cf. Scheme 1), or something else, such as some kind of bioelectrochemical stimulation of enzyme activities. The data processing by Faraday's law shows that in the case of biodegradation of 1,2-DBE the calculated degraded amounts by the measured electric current are comparable to the determined ones by chemical analyses. It means that there is an electrochemical component in the enhanced biodegradation or consecutive anode oxidation of 2-bromoethanol to bromo-acetaldehyde and mono-bromoacetic acid cf. Scheme 1.

It is interesting to find out the reasons for this effect. The first step for clarification of the mechanism of this enhanced biodegradation is the mathematical processing of the experimental data by unstructured models. A reasonably good fit of experimental data

with the modeling results will be an indication of the adequacy of the model presumptions and for clarification of the nature of the constant electric field impact by comparison of the evaluated kinetic constants in the used models. This impact can be on microbial growth and the associated growth inhibition by intermediate products, on the yields of biomass and products, the enhanced product oxidation, etc. The comparison of the estimated kinetic parameters by mathematical processing of the experimental data obtained with and without the application of a constant electric field can give an answer to these questions. The present paper is an attempt to evaluate these effects by means of mathematical models by processing the experimental data on 1,2-DBE biodegradation obtained with and without the application of the electric field.

We shall consider the case of 1,2-DBE biodegradation by the strain *Bradyrhizobium japonicum* 273 in the constant electric field at constant anode potential and for cases when no electric field was applied. The experimental data will be processed by two kinetic mathematical models to establish the reasons for the effect of the constant electric field for the considered case.

2. Materials and Methods

2.1. Bacterial Strain, Media and Experimental Conditions

The strain *Bradyrhizobium japonicum* 273 was obtained from the National Bank for Industrial Microorganisms and Cell Cultures, Bulgaria (NBIMCC). The strain was grown in mineral medium (MMY) containing (per liter): 1 g of yeast extract, 0.2 g of NaCl, 0.2 g of MgSO₄, 0.5 g of K₂HPO₄, 10 g of Glucose, and 1 L of tap water. The medium pH was adjusted to 7.2 before being autoclaved.

The experiments have been carried out under batch conditions in a 0.5 L Bioflo fermentor (New Brunswick Scientific, Edison, NJ, USA). The installation was loaded with substrate solution in nutritive medium and inoculum, which was 10% of the reactor volume, i.e., 50 mL. Temperature was measured by thermocouple and it is maintained constant at 30 °C by thermostat. The agitation speed of 400 rpm by magnetic stirrer was maintained constant. Processes of dehalogenation have been carried out with different initial substrate concentrations (0.05, 0.1, and 0.15 g/L) 1,2-DBE in presence and absence of constant electric field. For experiments with electric field, we used the following experimental set-up (Figure 1).

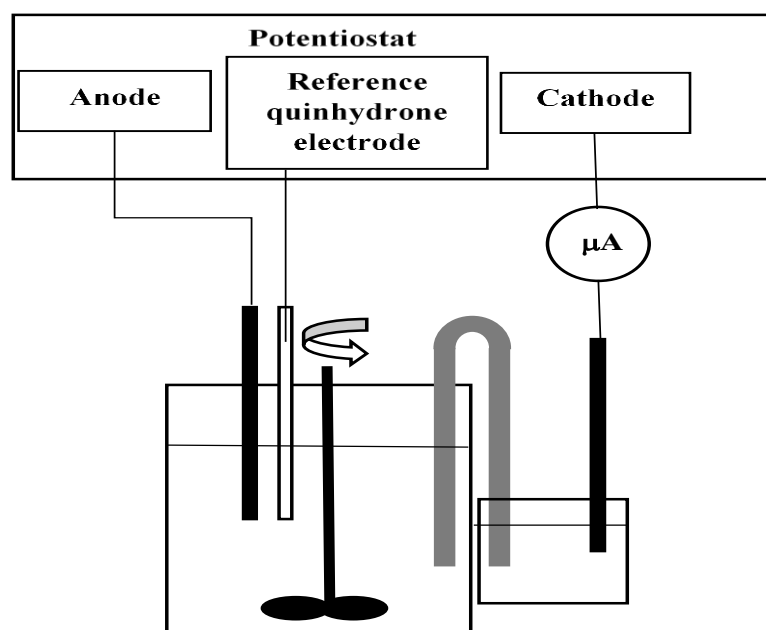


Figure 1. Experimental set-up with constant electric field application.

These experiments were made at three different anode potentials: 0.05, 0.1, and 0.15 V vs. reference quinhydrone electrode. Best results have been obtained at 0.1 V vs. the reference quinhydrone electrode. Therefore, our further considerations will be limited to this value of anode potential.

When applying electric field, one of the stainless steel baffles of the fermentor was used as an anode (with surface of 13 cm²). The anode potential was maintained constant by a potentiostat at the value of 0.1 V vs. quinhydrone electrode, (i.e., 0.8 V/SHE) at 30 °C. The abbreviation SHE denotes standard hydrogen electrode.

The cathode was coupled to the system by an agar salt bridge, outside the fermentor, in order to avoid undesired cathode processes in the broth. One end of the salt bridge was submerged in a beaker with sodium chloride solution, while the other end was submerged in the fermentor. The salt bridge was made of KCl and agar. At this temperature, the operating cell voltage was +0.6029 V. The current strength was measured by microammeter.

2.2. Analytical Methods

Samples from the broth were taken periodically and analyzed for biomass, 2-bromoethanol, and bromide ions. The biomass growth was monitored by the optical density of the broth. The light absorption was measured at a wavelength of 600 nm using a spectrophotometer. Calibration line was drawn by measuring the optical densities of dried samples of centrifuged biomass.

Bromides were analyzed by the colorimetric method of Bergman and Sanik, 1957 [19]. An aliquot of centrifuged sample (2.5 mL) was mixed with 1 mL of Fe (III) solution (8 g (NH₄)Fe(SO₄)·12H₂O in 100 mL of 6 M HNO₃) and 3 mL saturated solution of 1.5 g Hg(SCN)₂ in 500 mL of 98% ethanol. The mixture was shaken and after 10 min was filtered through a 0.2 μm filter. The light absorption was measured at a wavelength of 460 nm using a spectrophotometer. The concentrations of bromide ions were calculated from the optical density, using a calibration curve with correlation coefficient R² = 0.9996.

The presence of aldehydes was monitored qualitatively by the reaction of 2,4-dinitrophenylhydrazine (2,4-DNPH) with aldehydes. Carboxylic acids were monitored by HPLC.

In all photometrical determination, a UV-Vis spectrophotometer UV-1600 PC (a Shanghai Mapada Instruments Co. production, Shanghai, China) was used.

2.3. Mathematical Modeling

In this research, mathematical models of 1,2-dibromoethane biodegradation were composed. The used mathematical models are based on two kinetics of microbial growth involving competitive product inhibition. The first model is based on microbial growth, described by modified Monod equation for the specific growth rate [20]. The second one is based on inhibited growth by the product described by Levenspiel-type kinetics [21].

For the purpose of the modeling, own experimental data were used [17,18]. The effect of the electric field was estimated by the kinetic constants in the models for different initial substrate concentrations. Complete biodegradation was observed in cases of electric field application.

The mathematical description of the biodegradation process, using the modified Monod equation for the specific growth rate proposed by Yerusalmiskii and Neronova [20], has the form:

$$\begin{aligned} \frac{dX}{dt} &= \mu X, \mu = \mu_{max} \frac{S}{k_S + S} \frac{k_P}{k_P + P} \\ \frac{dS}{dt} &= -\frac{1}{Y_{X/S}} \mu X \\ \frac{dP}{dt} &= \frac{Y_{P/X}}{Y_{X/S}} \mu X - \gamma P \\ \frac{dBr}{dt} &= 0.63971 \left(\frac{Y_{P/S}}{Y_{X/S}} \mu X + \gamma P \right) \\ t = 0, X &= X_0, S = S_0, P = P_0, Br = Br_0 \end{aligned} \quad (1)$$

The second model equations are based on inhibited growth by the product described by Levenspiel-type kinetics [21]:

$$\begin{aligned} \frac{dX}{dt} &= \mu X, \mu = \mu_{max} \frac{S}{k_S + S} \left(1 - \frac{P}{P_{crit}}\right) \left(1 - \frac{P}{P_{crit}}\right)^n \\ \frac{dS}{dt} &= -\frac{1}{Y_{X/S}} \mu X \\ \frac{dP}{dt} &= \frac{Y_{P/X}}{Y_{X/S}} \mu X - \gamma P \\ \frac{dBr}{dt} &= 0.63971 \left(\frac{Y_{P/S}}{Y_{X/S}} \mu X + \gamma P\right) \\ t = 0, X &= X_0, S = S_0, P = P_0, Br = Br_0 \end{aligned} \quad (2)$$

where P_{crit} is a critical product concentration above which no growth is possible. In addition to product inhibition, the latter equation introduces product toxicity by the limiting value of P_{crit} . All used symbols are listed at the end of the paper.

The number 0.63971 is the stoichiometric ratio between the atomic mass of bromine and the molecular mass of 2-bromoethanol.

We did not detect aldehydes or carboxylic acids in the samples of the broth. An explanation for 1,2-DBE biodegradation, in this case, is the validity of a second mechanism of oxidative biodegradation, i.e., 2-bromoethanol is directly converted into ethylene oxide and further mineralized [11]. In any case, we restricted ourselves to evaluation of depletion of the first product, i.e., 2-bromoethanol to all other products in Scheme 1. Next, 2-bromoethanol will be considered the main inhibitor of bacterial growth.

The minimization of the least square function will be used for parameter identification.

There are six parameters for evaluation:— μ_{max} , k_S , $Y_{X/S}$, $Y_{P/S}$, k_P , and γ for the system (1) and seven for the Levenspiel model: μ_{max} , k_S , $Y_{X/S}$, $Y_{P/S}$, P_{crit} , n , and γ , cf. Equation (2). For this purpose of the experiment, experimental data were processed by minimization procedure of the target function Q , being the sum of the squares of the differences between the measured biomass and bromide concentrations (X^{exp} and Br^{exp}) and the model values:

$$Q = \sum_{i=0}^m \left[\left(X_i - X_i^{exp} \right)^2 + \left(Br_i - Br_i^{exp} \right)^2 \right] \quad (3)$$

where $i = 1, 2, 3, \dots, m$ are the numbers of the taken samples at moments t_i of the experiments. The concentration of the bromide anions is an indication of the progress of the substrate and product biodegradation. The attainment of a stoichiometric concentration of bromide in the broth means total conversion of 1,2-1,2-DBE to glycolic acid.

Model parameters identification in this case is a difficult task, because of the multi-extremal least square function or because some minima are ravine type. The solution to the problem needs very well parameter initial value approximations (in the global minimum area) for minimum searching procedure. This is the main problem in the multi-extremal function minimization is solved on the base of a hierarchical approach by using the experimental data or its spline approximations for solutions to the model equations [22]. In the present case, the identification problem for the biodegradation systems (1, 2) is solved using real experimental data [17,18].

A polynomial approximation of the experimental data is used for obtaining good initial values for the kinetic parameters (in the global minimum area) for the least square function minimization. The determination of the model parameters was made by minimization of the function, Equation (3) using the procedure `fminsearch` of MATLAB. This procedure finds minimum of unconstrained multivariable function using derivative-free method by algorithm "Nelder-Mead simplex direct search" [23].

3. Results

3.1. Experimental Data

An illustration of the positive effect of the applied electric field on bromide release and 2-bromoethanol depletion is shown in Figure 2.

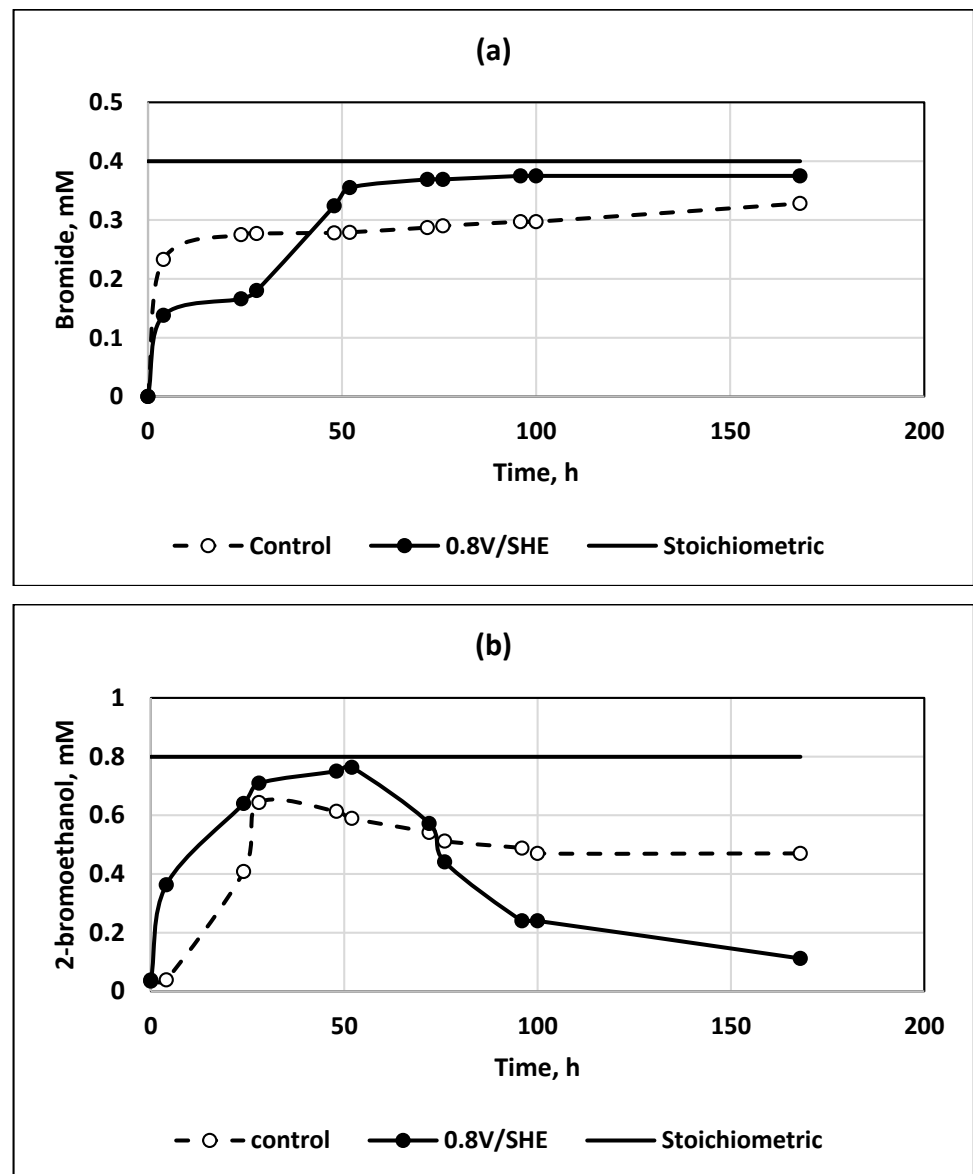


Figure 2. Experimental data for bromide release (a) and 2-bromoethanol formation and depletion (b) with and without electric field. Initial 1,2-DBE concentration 0.15 g dm^{-3} ; anode potential 0.8 V/SHE .

It is visible, that when electric field was applied bromide and 2-bromoethanol approached their stoichiometric values with much faster depletion of 2-bromoethanol. In the control experiment, its concentration remains constant for a long time.

3.2. Mathematical Modeling

The model curves for biomass growth and bromine release are almost identical for both models with the corresponding set of determined kinetic parameters. The obtained results for the values of kinetic parameters in models (3) and (4) for experiments with and without an electric field for two initial substrate concentrations are shown in Tables 1 and 2.

Table 1. The estimated data for the kinetic parameters in the models of product inhibition of microbial growth (1) and (2) without electric field for three initial concentrations of 1,2-dibromoethane.

Monod–Yerusalimsky, Equation (1)				Levenspiel, Equation (2)			
Initial Concentration, g dm ⁻³	0.05	0.1	0.15	Initial Concentration, g dm ⁻³	0.05	0.1	0.15
μ_{max} , h ⁻¹	0.3528	0.4167	0.4120	μ_{max} , h ⁻¹	0.4051	0.4070	0.4284
k_S , g dm ⁻³	0.4789	0.7061	0.7428	k_S , g dm ⁻³	0.5239	0.6515	0.6672
k_P , g dm ⁻³	0.2816	0.3705	0.3514	P_{crit} , g dm ⁻³	0.4432	0.4939	0.5068
$Y_{X/S}$, [-]	0.0859	0.1634	0.2532	$Y_{X/S}$, [-]	0.0842	0.1842	0.2489
$Y_{P/S}$, [-]	0.5357	0.6068	0.4719	$Y_{P/S}$, [-]	0.5655	0.6063	0.5120
γ , h ⁻¹	0.0011	0.0016	0.0014	γ , h ⁻¹	0.0016	0.0012	0.0013
				n	0.4431	0.4421	0.4431
Q_{min} , (g dm ⁻³) ²	8.4×10^{-5}	6.9×10^{-5}	3.2×10^{-4}	Q_{min} , (g dm ⁻³) ²	4.2×10^{-5}	6.9×10^{-5}	2.2×10^{-5}

Table 2. The estimated data for the kinetic parameters in the models of product inhibition of microbial growth (1) and (2) with electric field application at anode potential 0.8 V/SHE for three initial concentrations of 1,2-dibromoethane.

Monod–Yerusalimsky, Equation (1)				Levenspiel, Equation (2)			
Initial Concentration, g dm ⁻³	0.05	0.1	0.15	Initial Concentration, g dm ⁻³	0.05	0.1	0.15
μ_{max} , h ⁻¹	0.4056	0.4690	0.4818	μ_{max} , h ⁻¹	0.4237	0.4550	0.4635
k_S , g dm ⁻³	0.5106	0.7388	0.7696	k_S , g dm ⁻³	0.5521	0.7289	0.6873
k_P , g dm ⁻³	0.3205	0.4016	0.4181	P_{crit} , g dm ⁻³	0.4557	0.4905	0.5108
$Y_{X/S}$, [-]	0.1485	0.1878	0.2693	$Y_{X/S}$, [-]	0.1821	0.2013	0.2633
$Y_{P/S}$, [-]	0.6077	0.6368	0.5721	$Y_{P/S}$, [-]	0.5909	0.6389	0.6204
γ , h ⁻¹	0.0026	0.0025	0.0018	γ , h ⁻¹	0.0021	0.0022	0.0016
				n	0.4459	0.4448	0.4485
Q_{min} , (g dm ⁻³) ²	8.3×10^{-5}	3.5×10^{-5}	8.7×10^{-5}	Q_{min} , (g dm ⁻³) ²	4.1×10^{-5}	5.2×10^{-5}	7.5×10^{-5}

In all the cases the minimum sums of the squares Q_{min} were quite low and comparable for both models. That is why it is difficult to judge previously which model was more suitable to describe the studied processes.

The standard deviations calculated by the sums of the squares are less than 0.003 g dm⁻³. Note that the measured concentrations of bromide and 2-bromoethanol are within 0.05 to 0.09 g dm⁻³.

In the control experiments, the estimated maximum growth rates are almost equal for both models. The calculation shows for $\mu_{max} = (0.39 \pm 0.04) \text{ h}^{-1}$. The other common parameters, i.e., the saturation constant k_S , the yield coefficients $Y_{X/S}$ and $Y_{P/S}$ are also similar and the product yield coefficient is approaching its stoichiometric value, i.e., the ratio of the molecular masses of 2-bromoethanol and 1,2 dibromoethane, namely 0.665. The best results for the effect of an electric field are obtained at an initial concentration of 0.1 g dm⁻³.

The estimated rate constant γ for the product decay takes almost equal values by the two kinetic models.

On the other hand, it is evident that for the model of Monod–Yerusalimsky the effect of the electric field is strong for the maximum specific growth rate, for the growth inhibition constant k_P , for the product yield coefficient $Y_{P/S}$, and particularly for the rate constant for the product decay γ .

The data obtained by the Levenspiel model shows similar results for the maximum specific growth rate, the product yield coefficient, and the rate constant of the product decay except for the ones for the product inhibition. The values of the critical product concentration, P_{crit} , beyond which no microbial growth exists are practically equal for both cases. Next, the powers n are also too close considering the estimated scatter. Numerical computation of the product inhibition term in Equation (2) for the highest substrate concentration shows that there is negligible difference in their numerical values for the cases with and without electric field application, i.e., Levenspiel's model cannot distinguish the product inhibition for these two cases.

One more general conclusion can be drawn. That is, the main effect of the electric field is due to the increase in product depletion rate, γ . It is evident in both kinetic models. Obviously, it reflects on the product yield coefficient, even when the product inhibition on microbial growth is not pronounced, cf. the data for Levenspiel's model.

3.3. Experimental Data and Model Curves

A comparison of the experimental data and the model curves according to the Monod–Yerusalimsky model for microbial growth with and without the electric field for an initial concentration of 0.15 g dm^{-3} is shown in Figure 3. It is seen that in the case of electric field stimulation the steady state in microbial growth is attained at about the 70th hour, whereas it is attained at the 90th hour in the control experiment. A similar result is obtained at an initial concentration of 0.1 g dm^{-3} .

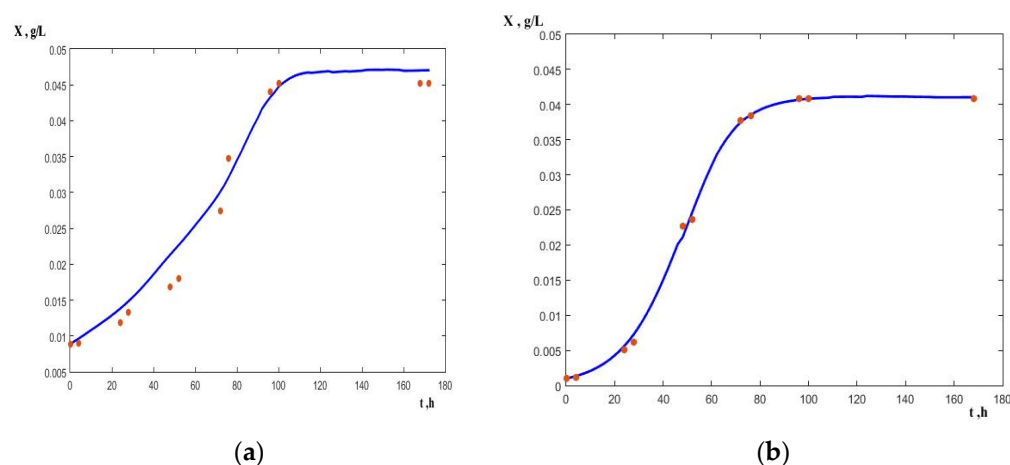


Figure 3. Comparison of the microbial growth rate with the model curves at initial substrate concentration 0.15 g dm^{-3} . The Monod–Yerusalimsky model (2); (a) control experiment with no electric field application; (b) data obtained at anode potential of 0.8 V/S.H.E.

A comparison of the model curves with the experimental data for bromide release is shown in Figures 4 and 5. The review of the experimental data in Figure 4 shows that the release of the second bromine atom is retarded in the control run (Figure 4a) compared to the one with an electric field (Figure 3b). At the initial substrate concentration of 0.1 g dm^{-3} , the release of the first bromine atom, (i.e., the complete depletion of the substrate) ends approximately at the 52nd hour in the control run with a bromide concentration of 0.0423 g dm^{-3} , whereas the release of the second one reached 0.0525 g dm^{-3} to the 170th hour. As a reference, the stoichiometric bromide concentration after complete dehalogenation must be 0.085 g dm^{-3} for this initial concentration.

When the electric field was applied, the release of the first bromine atom ended at the 4th hour at the same initial concentration, cf. Figure 4b. The second bromine atom was almost completely released at the 172nd hour (bromide concentration reached 0.072 g dm^{-3}) whereas it did not happen in the control experiment.

These effects are not so evident at the higher substrate concentration, i.e., 0.15 g dm^{-3} . Probably, it is because of the stronger product inhibition, cf. Figure 5. The first bromine atom was not completely released in the control experiment where the bromine concentration reached 0.0525 g dm^{-3} (Figure 5a). At this initial substrate concentration, a complete release of the first bromine atom the bromide concentration must be 0.064 g dm^{-3} . It was attained at the 80th hour when the electric field was applied, Figure 5b.

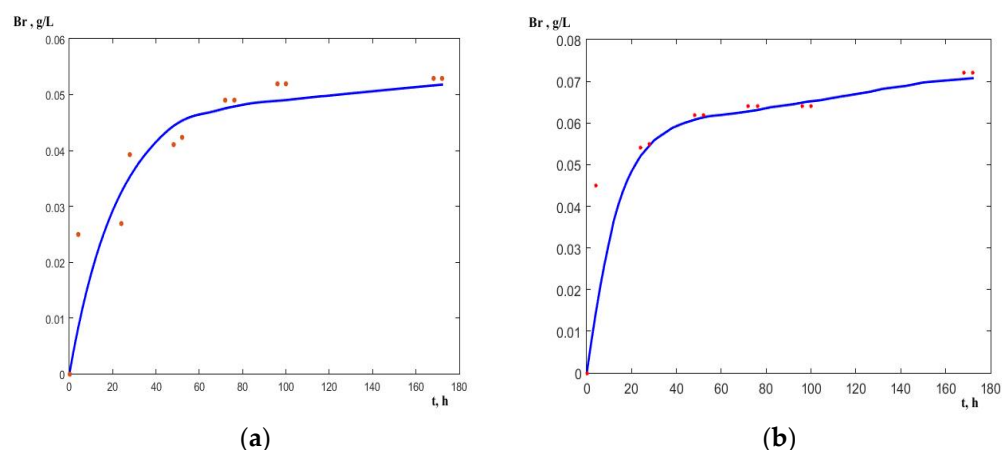


Figure 4. Comparison of the model curves for bromide concentration with experimental data. The Monod–Yerusalimsky model (2). Initial substrate concentration 0.1 g dm^{-3} . (a)—Control experiment with no electric field application; (b)—data obtained at anode potential of 0.8 V/S.H.E.

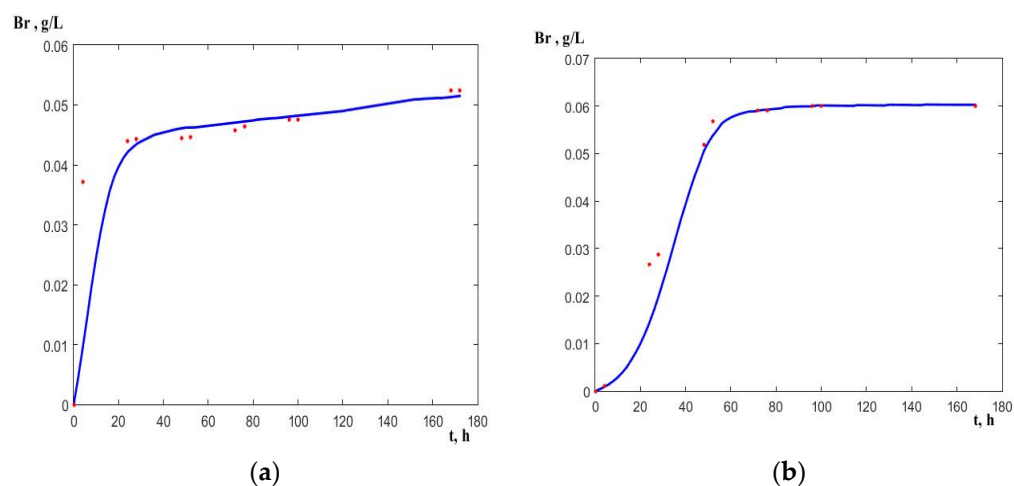


Figure 5. Comparison of the model curves for bromide concentration with experimental data. The Monod–Yerusalimsky model (2). Initial substrate concentration 0.15 g dm^{-3} . (a) Control experiment with no electric field application; (b) data obtained at anode potential of 0.8 V/S.H.E.

The release of the second bromine atom was strongly impeded at this initial concentration of 1,2 = dibromoethane. It corresponds to the lower values of the rate of product decay coefficient γ for this initial concentration, cf. Tables 1 and 2.

4. Discussion

A comparison of averaged values of the estimated parameters for the studied concentrations by the two models is shown in Table 3. The data scatter shows in which cases we can consider the effect of the electric field as significant and when, in case of scattering overlapping, such an effect is not significant.

There is a clear effect of the electric field on the kinetic constants determined by the use of both models, cf. Table 3. The main effects are in the maximum specific growth rate, $\mu_{\max} = (0.45 \pm 0.012) \text{ h}^{-1}$. It is approximately 12% higher than in the case of no electric field application. The effect of the electric field on the inhibition constant, estimated by the model of Monod–Yerusalimsky is also better pronounced.

Table 3. Comparison of the averaged values of estimated parameters for the two used kinetic models.

Monod–Yerusalimsky, Equation (1)			Levenspiel, Equation (2)		
Parameter	No Field	Electric Field, 0.8 V/SHE	Parameter	No Field	Electric Field, 0.8 V/SHE
μ_{max}, h^{-1}	0.39 ± 0.04	0.45 ± 0.04	μ_{max}, h^{-1}	0.41 ± 0.01	0.45 ± 0.02
$k_S, \text{g dm}^{-3}$	0.64 ± 0.14	0.67 ± 0.14	$k_S, \text{g dm}^{-3}$	0.61 ± 0.08	0.66 ± 0.09
$k_P, \text{g dm}^{-3}$	0.33 ± 0.05	0.38 ± 0.05	$P_{crit}, \text{g dm}^{-3}$	0.48 ± 0.03	0.49 ± 0.03
$Y_{X/S}, [-]$	0.17 ± 0.08	0.20 ± 0.06	$Y_{X/S}, [-]$	0.17 ± 0.08	0.22 ± 0.04
$Y_{P/S}, [-]$	0.54 ± 0.07	0.61 ± 0.03	$Y_{P/S}, [-]$	0.56 ± 0.05	0.62 ± 0.02
γ, h^{-1}	0.0014 ± 0.0003	0.0022 ± 0.0004	γ, h^{-1}	0.0014 ± 0.0002	0.0020 ± 0.0003
			n	0.443 ± 0.001	0.446 ± 0.002

Some of the estimated parameters are not affected by the electric field. They are the saturation constants k_S for both of the used models, the yield biomass coefficients $Y_{X/S}$, the critical product values, and the exponent n for the Levenspiel model. The overlapping of the scatters for these estimated parameters shows that there are no significant differences between the ones estimated for the control experiments and those obtained at the applied constant electric field.

The most significant effect of the electric field is the rate constant for the product decay γ . It is from 23 to 236% higher than in the control experiments with the highest value estimated by the Monod–Yerusalimsky model at an initial substrate concentration of 0.05 g dm^{-3} .

There is also a strong effect on the product yield coefficient $Y_{P/S}$, tending to reach the stoichiometric value of 0.665 for an initial concentration of 0.1 g dm^{-3} when the electric field is applied.

5. Conclusions

The mathematical modeling of experimental data for 1,2-dibromoethane biodegradation in a constant electric field by bacterial cells of *Bradyrhizobium japonicum* 273 shows that the main effect of the electric field is due to the enhanced product removal from the broth by electrochemical oxidation. This product, namely 2-bromoethanol, is an inhibitor and its removal facilitates microbial growth and the substrate to product conversion, reaching a yield coefficient close to the stoichiometric one.

In the considered case, the Monod–Yerusalimsky model is more sensitive to the evaluation of the effect of the electric field on microbial growth inhibition than the model of Levenspiel.

Based on the obtained results of mathematical modeling one can draw the following conclusions.

One of the most sensitive effects of the constant electric field on biodegradation of 1,2-bromoethanol is the enhancement of microbial growth, expressed by the increase in the maximum specific growth rate μ_{max} and the increase in the inhibition constant when the model of Monod–Yerusalimsky is applied.

The main effect of the electric field is in the increase in the rate constant of 2-bromoethanol removal by electrochemical oxidation, enabling the enhancement the microbial growth and substrate conversion to the product. Next, the oxidation of 2-bromoethanol results in almost complete substrate depletion with the release of bromine.

The model of Levenspiel is not so sensitive to the effects of the electric field on production inhibition and the electrochemical oxidation of 2-bromoethanol.

This approach of mathematical processing of experimental data of fermentation processes can be successfully applied for determining the microbial growth pattern and inhibition processes caused by higher substrate concentrations, based on the selected mathematical models.

Author Contributions: Conceptualization, V.B.; methodology, V.B.; software, P.P.-K.; validation, V.B. and P.P.-K.; formal analysis, investigation, E.V. and T.P.-M., data curation, E.V. and T.P.-M.; writing—original draft preparation, V.B.; writing and editing, V.B.; project administration, V.B.; funding acquisition, V.B. All authors have read and agreed to the published version of the manuscript.

Funding: This research was funded by the Fund for Scientific Research, Republic of Bulgaria, grant number DN 17/4/2017.

Institutional Review Board Statement: Not applicable.

Informed Consent Statement: Not applicable.

Data Availability Statement: Not applicable.

Acknowledgments: In this section, you can acknowledge any support given which is not covered by the author contribution or funding sections. This may include administrative and technical support, or donations in kind, (e.g., materials used for experiments).

Conflicts of Interest: The authors declare no conflict of interest.

Nomenclature

Br	Bromide concentration, g dm^{-3}
k_S	Saturation constant in the Monod equation, g dm^{-3}
kp	Inhibition constant, g dm^{-3}
n	Dimensionless power
P	The product concentration, i.e., 2-bromoethanol, g dm^{-3}
P_{crit}	Is a critical product concentration
Q	Target function, sum of least squares, Equation (3), $(\text{g dm}^{-3})^2$
S	Substrate (1,2-dibromoethane) concentration, g dm^{-3}
X	Biomass (microbial cell) concentration, g dm^{-3}
$Y_{P/S}$	Product yield coefficient, g/g
$Y_{X/S}$	Biomass yield coefficient, g/g
Greek symbols	
γ	Rate constant for 2-bromoethanol decay, h^{-1} .
μ	The specific microbial growth rate, h^{-1}
μ_{max}	Maximum specific microbial growth rate, h^{-1}

References

- Falta, R.W.; Bulsara, N.; Henderson, J.K.; Mayer, R.A. Leaded-gasoline additives still contaminate groundwater. *Environ. Sci. Technol.* **2005**, *39*, 378A–384A. [CrossRef] [PubMed]
- Alexeeff, G.V.; Kilgore, W.W.; Li, M.Y. Ethylene dibromide: Toxicology and risk assessment. *Rev. Environ. Contam. Toxicol.* **1990**, *112*, 49–122. [PubMed]
- Pignatello, J.J. Microbial degradation of 1,2-dibromoethane in shallow aquifer materials. *J. Environ. Qual.* **1987**, *16*, 307–312. [CrossRef]
- Steinberg, S.M.; Pignatello, J.J.; Sawhney, B.L. Persistence of 1,2-dibromoethane in soils: Entrapment in intraparticle micropores. *Environ. Sci. Technol.* **1987**, *21*, 1201–1208. [CrossRef]
- Hatzinger, P.; Begley, J.; Lippincott, D.; Bodour, A.; Forbes, R. In situ bioremediation of 1,2-dibromoethane (1,2-DBE) in groundwater to part per-trillion concentrations using co-metabolism. *J. Contam. Hydrol.* **2018**, *218*, 120–129. [CrossRef] [PubMed]
- McKeever, R.; Sheppard, D.; Nuesslein, K.; Baek, K.-H.; Rieber, K.; Ergas, S.J.; Forbes, R.; Hilyard, M.; Park, C. Biodegradation of ethylene dibromide (1,2-dibromoethane 1,2-DBE) in microcosms simulating in situ and biostimulated conditions. *J. Hazard. Mater.* **2012**, *209*, 92–98. [CrossRef]
- Huff, J.E. 1,2-Dibromoethane (ethylene dibromide). *Environ. Health Perspect.* **1983**, *47*, 359–363. [CrossRef]
- Hill, D.L.; Shih, T.-W.; Johnston, T.P.; Struck, R.F. Macromolecular binding and metabolism of the carcinogen 1,2-dibromoethane. *Cancer Res.* **1978**, *38*, 2438–2442.
- Falta, R.W. The potential for ground water contamination by the gasoline lead scavengers ethylene dibromide and 1,2-dichloroethane. *Groundw. Monit. Remediat.* **2004**, *24*, 76–87. [CrossRef]
- Agency for Toxic Substances and Disease Registry. *ToxFAQs for 1,2-Dichloroethane and 1,2-Dibromoethane*; Agency for Toxic Substances and Disease Registry: Atlanta, GA, USA, 1995. Available online: <http://www.atsdr.cdc.gov/tfacts37.pdf> (accessed on 4 April 2022).
- Freitas dos Santos, L.M.; Leak, D.J.; Livingston, A.G. Enrichment of mixed cultures capable of aerobic degradation of 1,2-dibromoethane. *Appl. Environ. Microbiol.* **1996**, *62*, 4675–4677. [CrossRef]

12. Poelarends, G.J.; van Hylckama Vlieg, J.E.T.; Marchesi, J.R.; Freitas Dos Santos, L.M.; Janssen, D.B. Degradation of 1,2-dibromoethane by *Mycobacterium* sp. strain GP1. *J. Bacteriol.* **1999**, *181*, 2050–2058. [CrossRef] [PubMed]
13. Janssen, D.B.; Pries, F.; van der Ploeg, J. Genetics and biochemistry of dehalogenating enzymes. *Ann. Rev. Microbiol.* **1994**, *48*, 163–191. [CrossRef] [PubMed]
14. van der Ploeg, J.; Willemsen, M.; van Hall, G.; Janssen, D.B. Adaptation of *Xanthobacter autotrophicus* GJ10 to bromoacetate due to activation and mobilization of the haloacetate dehalogenase gene by insertion element IS1247. *J. Bacteriol.* **1995**, *177*, 1348–1356. [CrossRef] [PubMed]
15. Tandol, V.; DiStefano, T.D.; Bowser, P.A.; Gosset, J.M.; Zinder, S.H. Reductive dehalogenation of chlorinated ethenes and halogenated ethenes by a high-rate anaerobic enrichment culture. *Environ. Sci. Technol.* **1994**, *28*, 973–979. [CrossRef]
16. Skopelitou, K.; Georgakis, N.; Efroze, R.; Flemetakis, E.; Labrou, N. Sol-gel immobilization of haloalkane dehalogenase from *Bradyrhizobium japonicum* for the remediation 1,2-dibromoethane. *J. Mol. Catalysis B Enzym.* **2013**, *97*, 5–11. [CrossRef]
17. Vasileva, E.; Parvanova-Mancheva, T.; Beschkov, V. 1,2-Dibromoethane biodegradation capacity of *Bradyrhizobium japonicum* strain 273. *J. Int. Sci. Publ. Ecol. Safety* **2018**, *12*, 82–89. Available online: <http://www.scientific-publications.net> (accessed on 1 October 2018).
18. Vasileva, E.; Parvanova-Mancheva, T.; Beschkov, V. Biodegradation of 1,2-dibromoethane by *Bradyrhizobium japonicum* 273 strain by free and immobilized cells stimulated by constant electric field. *J. Int. Sci. Publ. Mater. Methods Technol.* **2019**, *13*, 99–109.
19. Bergmann, J.G.; Sanik, J. Determination of trace amounts of chlorine in naphtha. *Anal. Chem.* **1957**, *29*, 241–243. [CrossRef]
20. Yeruslimsky, N.D.; Neronova, N.M. Quantitative relationships between metabolic products and growth rate of microorganisms. *Doklad Akademii Nauk USSR* **1965**, *161*, 1437–1440. (In Russian)
21. Levenspiel, O. The Monod equation. A revisit and a generalization to product inhibition situation. *Biotechnol. Bioeng.* **1980**, *22*, 1671–1687. [CrossRef]
22. Popova-Krumova, P.; Boyadjiev, C. Approach for parameter identification of multiparameter models. In *Modeling and Simulation in Chemical Engineering, Project Reports on Process Simulation*, 1st ed.; Boyadjiev, C., Ed.; Book Series: Heat and Mass Transfer; Springer Nature Switzerland AG: Cham, Switzerland, 2021; pp. 147–154.
23. Lagarias, J.C.; Reeds, J.A.; Wright, M.H.; Wright, P.E. Convergence properties of the Nelder-Mead simplex method in low dimensions. *SIAM J. Optim.* **1998**, *9*, 112–147. [CrossRef]